Mon. Not. R. Astron. Soc. **000**, 000–000 (1996) Printed February 1, 2008

The Persistence of Warps in Spiral Galaxies with Massive Halos

James Binney, Ing-Guey Jiang and Suvendra Dutta
Theoretical Physics, University of Oxford, Oxford, OX1 3NP

ABSTRACT
We study the persistence of warps in galactic discs in the presence of massive halos. A disc is approximated by a set of massive rings, while a halo is represented by a conventional n-body simulation. We confirm the conclusion of Nelson & Tremaine (1995) that a halo responds strongly to an embedded precessing disc. This response invalidates the approximations made in the derivation of classical 'modified tilt' modes. We show that the response of the halo causes the line of nodes of a disc that starts from a modified tilt mode to wind up within a few dynamical times. We explain this finding in terms of the probable spectrum of true normal modes of a combined disc–halo system.

Key words: Warps: galaxies

1 INTRODUCTION

At least 50 percent of spiral galaxies have warped discs, and it is likely that *all* galactic discs are slightly warped. Given the importance of the warp phenomenon and the fact that it is now nearly 40 years since the first warp, that of the Milky Way, was discovered, it is remarkable that there is still no generally accepted explanation of the phenomenon. Several recent reviews survey the literature of subject (e.g., Binney, 1992; Nelson & Tremaine, 1996).

To a first approximation most warped discs may be represented by an ensemble of rigid, concentric rings. Each ring is spinning and coupled to the other rings and to non-disc material by gravity. The gravitational torques on the rings cause their spin angular momenta to precess, and the fundamental problem posed by the phenomenon of warps is to understand how, despite this precession, the orientations of rings are coordinated, as they must be if the disc is to remain smooth and thin.

An explanation that has enjoyed considerable popularity is that the rings are sufficiently tightly coupled to one another by gravity that they can precess together in the non-spherical gravitational potential of a massive halo as if they formed a rigid body (Toomre 1983; Dekel & Shlosman 1983). Since in this model the height of the disc above the halo's equatorial plane varies sinusoidally in time, the disc is said to have an excited normal mode. The mode in question is a modification of a trivial zero-frequency solution of the linearized equations of motion of an isolated system of rings. This zero-frequency mode corresponds to a simple tilt of the system of rings with respect to the coordinate system employed. Hence it is called the 'modified tilt' mode of the disc. The modified tilt modes of discs were thoroughly studied by Sparke & Casertano (1988). They found that some well-observed warps could be successfully modelled by modified tilt modes.

Unfortunately, modified tilt modes are artificial in that they rest on the assumption that the halo potential, which is responsible for the precession of the disc, is unaffected by the disc's precession. In reality halo objects will tend to pick up energy from the time-varying potential of the disc, and any increase in the halo's energy is likely to be at the expense of the energy of the disc's modified tilt mode. Nelson & Tremaine (1995) estimated the rate of energy transfer from the disc to the halo and found it to be surprisingly large. They concluded that in realistic circumstances a modified tilt mode will be damped within one dynamical time of the disc.

In this paper we use numerical simulations to test and clarify the semi-analytic work of Nelson & Tremaine. What they calculated was the rate at which halo stars would acquire energy if (a) the warped disc precessed precisely as predicted by Sparke & Casertano, and (b) if the time-averaged potential governing the motion of halo particles is spherical. The latter assumption is obviously unphysical and imposed only in order to facilitate the calculations. However, intuitively one feels that the final result should not be sensitive to this assumption. By contrast the first assumption, that the disc precesses according to the prediction of Sparke & Casertano, is incompatible with the large energy transfer rate obtained by Nelson & Tremaine, since this demonstrates that effects neglected by Sparke & Casertano are in fact large.

Simulations of disc–halo interaction are demanding numerically because the scales of the disc and halo are very different. Some numbers appropriate to the Milky way will illustrate this. The disc scale length is $\sim 3\,$kpc (Kent, Dame & Fazio, 1991) while the halo probably extends at least to the galactocentric distance $r \simeq 50\,$kpc of the Magellanic Clouds (Fich & Tremaine, 1991). Moreover, it is essential for the halo mass and angular momentum to exceed those of the disc by a considerable factor. On the other hand, the

individual masses of halo particles should be smaller than those of disc particles in order that the halo's structure is sufficiently well defined in the neighbourhood of the disc. In particular, spurious stochastic acceleration of disc particles by halo particles must be avoided, as must significant two-body relaxation within the small fraction of the halo that lies within the disc. The difficulty of satisfying these conflicting requirements is illustrated by the simulations of Dubinski & Kuijken (1995). They simulated a disc–halo system with a direct n-body simulation in which 50 000 particles were assigned to the halo and 40 000 particles were assigned to the disc. Typically, their halo particles were *more* massive than their disc particles by a factor in excess of 6. In such a simulation the disc is inevitably so thick that one cannot meaningfully determine whether any warp's line of nodes is straight or has a tendency to wind up.

Here we represent only the halo by an n-body simulation, while modelling the embedded disc by a series of rigid concentric rings. The latter approximation to disc dynamics was introduced by Hunter & Toomre (1969) and has since been widely used in theoretical work. However, it does not seem before to have been directly coupled to an n-body simulation. It enables us to assign all our 100 000 particles to the halo and to have a well defined line of nodes in a disc whose 100 individual rings have masses that are larger than those of halo particles by a factor of 100.

In Section 2 we set out the equation of motion of the disc and halo system. In Section 3, we describe numerical details and the initial conditions we have used for the halo and the disc. In Section 4 we check that our simulations can reproduce previous results and go on to show that a dynamical halo causes a warp to wind up rapidly when it starts from the configuration of the modified tilt mode for the case of a frozen halo. In Section 5 we explain this result in terms of the probable normal-mode spectrum of the coupled disc–halo system.

2 FORMALISM

2.1 Disc dynamics

The equation of motion of a disc star is

$$\frac{\mathrm{d}^2z}{\mathrm{d}t^2} = -\frac{\partial\Phi_\mathrm{h}}{\partial z} + f, \tag{1}$$

where Φ_h is the gravitational potential of the halo and f is the vertical force on the particle from the disc. For small excursions out of the xy-plane, the halo term in (1) can be expanded as

$$\begin{aligned}\frac{\partial\Phi_\mathrm{h}}{\partial z} &= \frac{\partial\Phi_\mathrm{h}}{\partial z}\bigg|_{z=0} + z\frac{\partial^2\Phi_\mathrm{h}}{\partial z^2}\bigg|_{z=0} + \mathrm{O}(z^2)\\ &\simeq -(F_\mathrm{h} - \kappa_z^2 z),\end{aligned} \tag{2}$$

where

$$\begin{aligned}F_\mathrm{h} &\equiv -\partial\Phi_\mathrm{h}/\partial z|_{z=0}\\ \kappa_z^2 &\equiv \partial^2\Phi_\mathrm{h}/\partial z^2|_{z=0}.\end{aligned} \tag{3}$$

When we express the total time derivative in (1) in terms of partial derivatives we now have

$$\Big(\frac{\partial}{\partial t} + \Omega\frac{\partial}{\partial\phi}\Big)^2 z = F_\mathrm{h} - \kappa_z^2 z + f, \tag{4}$$

where $\Omega(r)$ is the circular frequency at radius r.

Following Hunter & Toomre (1969) we focus on the $m = 1$ distortions of the disc by assuming that z is of the form

$$z(t,r,\phi) = \sqrt{2}\big[z_\mathrm{c}(t,r)\cos(\phi) + z_\mathrm{s}(t,r)\sin(\phi)\big]. \tag{5}$$

With this assumption the disc may be considered to consist of a nested sequence of rigid rings. Then $\sqrt{2}z_\mathrm{c}(t,r)$ is the height at which the ring of radius r passes over the positive x-axis at time t, while $\sqrt{2}z_\mathrm{s}(t,r)$ is the height of the corresponding passage over the y-axis. (The factors of $\sqrt{2}$ will ensure that the expression for the energy of the warp is natural.) When we similarly decompose $F_\mathrm{h}(t,r,\phi)$ and $f(t,r,\phi)$ in the form (5), equation (4) yields coupled equations of motion for z_c and z_s:

$$\begin{aligned}\frac{\partial^2 z_\mathrm{c}}{\partial t^2} + 2\Omega\frac{\partial z_\mathrm{s}}{\partial t} - \Omega^2 z_\mathrm{c} &= F_\mathrm{hc} - \kappa_z^2 z_\mathrm{c} + f_\mathrm{c},\\ \frac{\partial^2 z_\mathrm{s}}{\partial t^2} - 2\Omega\frac{\partial z_\mathrm{c}}{\partial t} - \Omega^2 z_\mathrm{s} &= F_\mathrm{hs} - \kappa_z^2 z_\mathrm{s} + f_\mathrm{s}.\end{aligned} \tag{6}$$

We calculate the vertical forces between the rings to first order in z_c and z_s by splitting the force into two parts $f^{(a)}$ and $f^{(b)}$ (Toomre, private communication). $f^{(a)}$ is the force on a ring that lies in the xy-plane from other, tilted rings, while $f^{(b)}$ is the force on a tilted ring when the other rings lie in the xy-plane. For a ring of radius r, we have

$$\begin{aligned}f^{(a)}(r,\phi) &= \sum_{r'\neq r}\frac{Gm_{r'}}{2\pi}z(r',\phi)\int_{\theta=0}^{2\pi}\frac{\cos\theta\mathrm{d}\theta}{\Delta(r,r',\theta)},\\ f^{(b)}(r,\phi) &= -\sum_{r'\neq r}\frac{Gm_{r'}}{2\pi}z(r,\phi)\int_{\theta=0}^{2\pi}\frac{\mathrm{d}\theta}{\Delta(r,r',\theta)},\end{aligned} \tag{7a}$$

where $m_{r'}$ is the mass of the ring of radius r' and

$$\Delta(r,r',\theta) \equiv (r^2 + r'^2 + a^2 - 2rr'\cos\theta)^{3/2}. \tag{7b}$$

Here a is the softening of the force that arises because the disc has finite vertical thickness $\Delta z \simeq a$.

If Φ_d is the gravitational potential of the disc, the circular frequency Ω is given by

$$\begin{aligned}\Omega &= \sqrt{\frac{1}{r}\bigg(\frac{\partial\Phi_\mathrm{h}}{\partial r}\bigg|_{z=0} + \frac{\partial\Phi_\mathrm{d}}{\partial r}\bigg|_{z=0}\bigg)}\\ &\equiv \sqrt{\Omega_\mathrm{h}^2 + \Omega_\mathrm{d}^2}.\end{aligned} \tag{8}$$

By analogy with the vertical forces, we decompose Ω_d^2 into contributions that are proportional to the two integrals that appear in equations (7a):

$$\Omega_\mathrm{d}^2(r) = S^{(a)} + S^{(b)}, \tag{9}$$

where

$$\begin{aligned}S^{(a)}(r) &\equiv -\sum_{r'\neq r}\frac{r'}{r}\frac{Gm_{r'}}{2\pi}\int\frac{\cos\theta\mathrm{d}\theta}{\Delta(r,r',\theta)},\\ S^{(b)}(r) &\equiv \sum_{r'\neq r}\frac{Gm_{r'}}{2\pi}\int\frac{\mathrm{d}\theta}{\Delta(r,r',\theta)}.\end{aligned} \tag{10}$$

Hence we have finally that equations (6) may be written

$$\begin{aligned}\ddot{z}_{\mathrm{c}i} + 2\Omega_i \dot{z}_{\mathrm{s}i} - \Omega_i^2 z_{\mathrm{c}i} &= F_{\mathrm{hc}} - \kappa_{zi}^2 z_{\mathrm{c}i} \\ &\quad + \sum_j z_{\mathrm{c}j} f_{ij}^{(a)} + z_{\mathrm{c}i} \sum_j f_{ij}^{(b)} \\ \ddot{z}_{\mathrm{s}i} - 2\Omega_i \dot{z}_{\mathrm{c}i} - \Omega_i^2 z_{\mathrm{s}i} &= F_{\mathrm{hs}} - \kappa_{zi}^2 z_{\mathrm{s}i} \\ &\quad + \sum_j z_{\mathrm{s}j} f_{ij}^{(a)} + z_{\mathrm{s}i} \sum_j f_{ij}^{(b)}\end{aligned} \tag{11a}$$

where,

$$\begin{aligned} f_{ij}^{(a)} &\equiv \frac{Gm_j}{2\pi} \int_0^{2\pi} \frac{\cos\theta \mathrm{d}\theta}{\Delta(r_i, r_j, \theta)}, \\ f_{ij}^{(b)} &\equiv -\frac{Gm_j}{2\pi} \int_0^{2\pi} \frac{\mathrm{d}\theta}{\Delta(r_i, r_j, \theta)}. \end{aligned} \tag{11b}$$

Equations (11a) lead naturally to a definition of the warp's energy

$$E_{\mathrm{warp}} = \tfrac{1}{2} \sum_i m_i \dot{z}_i^2 + V_{\mathrm{dh}}^{\mathrm{w}} + V_{\mathrm{dd}}^{\mathrm{w}}, \tag{12}$$

where

$$\dot{z}_i^2 \equiv (\dot{z}_{\mathrm{c}i})^2 + (\dot{z}_{\mathrm{s}i})^2 \,. \tag{13}$$

and the two potential-energy terms are defined by

$$\begin{aligned} V_{\mathrm{dh}}^{\mathrm{w}} &\equiv \sum_{i=0}^{N_{\mathrm{r}}} m_i \left[\tfrac{1}{2} z_i^2 \left(\kappa_{zi}^2 - \Omega_{\mathrm{h}i}^2 \right) - \left(F_{\mathrm{hc}i} z_{\mathrm{c}i} + F_{\mathrm{hs}i} z_{\mathrm{s}i} \right) \right], \\ V_{\mathrm{dd}}^{\mathrm{w}} &\equiv -\tfrac{1}{2} \sum_i m_i \left[z_{\mathrm{c}i} \left(\sum_j z_{\mathrm{c}j} f_{ij}^{(a)} + z_{\mathrm{c}i} \sum_j f_{ij}^{(b)} \right) \right. \\ &\quad \left. + z_{\mathrm{s}i} \left(\sum_j z_{\mathrm{s}j} f_{ij}^{(a)} + z_{\mathrm{s}i} \sum_j f_{ij}^{(b)} \right) + \Omega_{\mathrm{d}i}^2 z_i^2 \right]. \end{aligned} \tag{14}$$

Here

$$z_i^2 \equiv z_{\mathrm{c}i}^2 + z_{\mathrm{s}i}^2. \tag{15}$$

2.2 The halo

We represent the halo by an ensemble of particles that move in the combined potential of the halo and disc. We expand this potential and the halo's density in spherical harmonics as follows,

$$\begin{aligned} \rho_{\mathrm{h}}(r, \theta, \phi) &= \sum_{l=0} \sum_{m=0}^{l} p_l^m(\cos\theta) \\ &\quad \times \left[A_{lm}(r) \cos(m\phi) + B_{lm}(r) \sin(m\phi) \right], \\ \Phi_{\mathrm{h}}(r, \theta, \phi) &= \sum_{l=0} \sum_{m=0}^{l} p_l^m(\cos\theta) \\ &\quad \times \left[C_{lm}(r) \cos(m\phi) + D_{lm}(r) \sin(m\phi) \right]. \end{aligned} \tag{16}$$

Here the p_l^m are defined in terms of the conventional Legendre functions P_l^m by

$$p_l^m \equiv \sqrt{\frac{(l-|m|)!}{(l+|m|)!}} P_l^m \tag{17}$$

and the C_{lm} are related to A_{lm} by

$$\begin{aligned} C_{lm}(r) &= C_{1lm}(r) + C_{2lm}(r) \\ C_{1lm}(r) &\equiv -\frac{4\pi G}{2l+1} r^{-l-1} \int_0^r \mathrm{d}s \, s^{l+2} A_{lm}(s) \\ C_{2lm}(r) &= -\frac{4\pi G}{2l+1} r^{l} \int_r^\infty \mathrm{d}s \, s^{1-l} A_{lm}(s). \end{aligned} \tag{18}$$

An expression for the D_{lm} in terms of the B_{lm} is obtained by replacing C with D and A with B in these expressions.

In the linear regime the vertical force on a ring is characterized by the force components,

$$\begin{aligned} F_{\mathrm{hc}}(r) &= \frac{1}{r} \sum_l \frac{\mathrm{d}p_l^1(\mu)}{\mathrm{d}\mu} \bigg|_{\mu=0} C_{l1} \\ F_{\mathrm{hs}}(r) &= \frac{1}{r} \sum_l \frac{\mathrm{d}p_l^1(\mu)}{\mathrm{d}\mu} \bigg|_{\mu=0} D_{l1} \end{aligned} \tag{19}$$

and by the frequency,

$$\kappa_z^2(r) = \sum_{l=0} \left(P_l(0) \frac{E_{l0}}{r} + \frac{\mathrm{d}^2 P_l(\mu)}{\mathrm{d}\mu^2} \bigg|_{\mu=0} \frac{C_{l0}}{r^2} \right), \tag{20}$$

where

$$E_{l0} \equiv -(l+1) \frac{C_{1l0}}{r} + l \frac{C_{2l0}}{r}. \tag{21}$$

The halo's contribution to the circular frequency is

$$\Omega_{\mathrm{h}}^2 = \frac{1}{r} \sum_{l=0} P_l(0) E_{l0}(r). \tag{22}$$

2.3 The coupling between disc and halo

The potential of a ring of radius r' may be written

$$\Phi(r, \theta, \phi) = \sum_{l=0} \Phi_l \zeta^l P_l(\cos\gamma), \tag{23a}$$

where the Φ_l are coefficients to be determined,

$$\zeta \equiv \frac{\min(r', r)}{\max(r', r)}, \tag{23b}$$

and γ is the angle between the ring's symmetry axis and the direction (θ, ϕ). On the ring's symmetry axis, $\gamma = 0$, we have

$$\begin{aligned} \Phi(r, \gamma = 0) &= -\frac{Gm_{r'}}{\sqrt{r'^2 + r^2}} \\ &= -\frac{Gm_{r'}}{\max(r', r)} \left(1 - \tfrac{1}{2}\zeta^2 + \tfrac{1.3}{2^2 2!}\zeta^4 - \cdots \right). \end{aligned} \tag{24}$$

Since $P_l(1) = 1$ for all l, the values of the Φ_l follow immediately from a comparison of equations (23a) and (24).

The addition theorem for associated Legendre functions may be written

$$\begin{aligned} P_l(\cos\gamma) = \sum_{m=0}^{l} \frac{2}{\epsilon_m^{\mathrm{c}}} p_l^m(\cos\theta_T) p_l^m(\cos\theta) \\ \times \cos\left[m(\phi - \phi_T) \right], \end{aligned} \tag{25a}$$

where γ is the angle between the general directions (θ_T, ϕ_T) and (θ, ϕ), and

$$\epsilon_m^{\mathrm{c}} \equiv \begin{cases} 2 & \text{for } m = 0, \\ 1 & \text{otherwise.} \end{cases} \tag{25b}$$

We set (θ_T, ϕ_T) equal to the polar angles of the ring's symmetry axis

$$\theta_T(r') = \sin^{-1}\left(\frac{\sqrt{2(z_{\rm c}^2+z_{\rm s}^2)}}{r'}\right), \qquad \phi_T(r') = \frac{\pi}{2} + \mathrm{atan2}\,(z_{\rm c}, -z_{\rm s})\,, \tag{26}$$

and eliminate $P_l(\cos\gamma)$ between equations (23a) and (25a):

$$\begin{aligned}\Phi(r,\theta,\phi) &= \sum_{l=0}\Phi_l\zeta^l\sum_{m=0}^{l}\frac{2}{\epsilon_m^{\rm c}}p_l^m(\cos\theta_T)p_l^m(\cos\theta)\\ &\qquad\times\cos[m(\phi-\phi_T)]\\ &= \sum_{l=0}\sum_{m=0}^{l}p_l^m(\cos\theta)\\ &\qquad\times[C'_{lm}\cos(m\phi)+D'_{lm}\sin(m\phi)],\end{aligned} \tag{27a}$$

where

$$\begin{aligned}C'_{lm}(r) &\equiv \frac{2}{\epsilon_m^{\rm c}}\Phi_l\zeta^l p_l^m(\cos\theta_T)\cos(m\phi_T),\\ D'_{lm}(r) &\equiv \frac{2}{\epsilon_m^{\rm c}}\Phi_l\zeta^l p_l^m(\cos\theta_T)\sin(m\phi_T).\end{aligned} \tag{27b}$$

2.4 Energy integrals

The potential energy of the system is $V = V_{\rm hh} + V_{\rm hd} + V_{\rm dd}$, where,

$$\begin{aligned}V_{\rm hh} &\equiv \tfrac{1}{2}\int {\rm d}^3\boldsymbol{r}\,\rho_{\rm h}\Phi_{\rm h},\\ V_{\rm hd} &\equiv \int {\rm d}^3\boldsymbol{r}\,\rho_{\rm h}\Phi_{\rm d} = V_{\rm dh} \equiv \int {\rm d}^2\boldsymbol{r}\,\Sigma_{\rm d}\Phi_{\rm h},\\ V_{\rm dd} &= \tfrac{1}{2}\int {\rm d}^2\boldsymbol{r}\,\Sigma_{\rm d}\Phi_{\rm d}.\end{aligned} \tag{28}$$

The requirement that $V_{\rm hd} = V_{\rm dh}$ provides a non-trivial check on the accuracy of the calculations.

2.4.1 Self potential energy of the halo

$V_{\rm hh}$ can be expressed in terms of the coefficients defined above of the spherical-harmonic expansions of $\rho_{\rm h}$ and $\Phi_{\rm h}$:

$$V_{\rm hh} = \sum_{l=0}\frac{\pi}{2l+1}\sum_{m=0}^{l}\int {\rm d}r\, r^2\left[\epsilon_m^{\rm c}A_{lm}C_{lm} + \epsilon_m^{\rm s}B_{lm}D_{lm}\right], \tag{29}$$

where $\epsilon_m^{\rm s} = 0$, if $m = 0$ and 1, otherwise.

2.4.2 Interaction of the halo and the disc

Similarly, the energy of interaction of disc and halo can be written

$$V_{\rm hd} = \sum_{l=0}\frac{2\pi}{2l+1}\sum_{m=0}^{l}\int {\rm d}r\, r^2\left(\epsilon_m^{\rm c}A_{lm}C'_{lm} + \epsilon_m^{\rm s}B_{lm}D'_{lm}\right). \tag{30}$$

We decompose $V_{\rm dh}$ into two parts, a part $V_{\rm dh}^{\rm u}$ associated with a flat disc that lies in the xy-plane, and a part $V_{\rm dh}^{\rm w}$ associated with warping or tilting of the disc. We have

$$V_{\rm dh}^{\rm u} = \int_0^\infty {\rm d}r\, r\int_0^{2\pi}{\rm d}\phi\,\Sigma_{\rm d}(r)\Phi_{\rm h}(r,0,\phi). \tag{31}$$

Setting

$$\Sigma_{\rm d}(r) = \sum_{i=0}^{N_{\rm r}} m_i\frac{\delta(r-r_i)}{2\pi r_i} \tag{32}$$

and using equation (16) we find

$$V_{\rm dh}^{\rm u} = \sum_{i=0}^{N_{\rm r}} m_i\sum_{l=0}P_l(0)C_{l0}(r_i). \tag{33}$$

We calculate $V_{\rm dh}^{\rm w}$ by substituting equation (32) into the (28) and expanding $\Phi_{\rm h}$ in cylindrical polar coordinates (R,ϕ,z):

$$\begin{aligned}V_{\rm dh}^{\rm w} &= \int {\rm d}^2\boldsymbol{r}\sum_{i=0}^{N_{\rm r}} m_i\frac{\delta(r-r_i)}{2\pi r_i}\Phi_{\rm h}(R,\phi,z)\\ \Phi_{\rm h}(R,\phi,z) &= \Phi_{\rm h}(r,\phi,0) + \frac{\partial\Phi_{\rm h}}{\partial R}\delta R + \frac{\partial\Phi_{\rm h}}{\partial z}z\\ &\qquad + \tfrac{1}{2}\frac{\partial^2\Phi_{\rm h}}{\partial z^2}z^2 + \cdots\\ &\simeq \Phi_{\rm h}(r,\phi,0) - \frac{z^2}{2r}\frac{\partial\Phi_{\rm h}}{\partial R} - H_{\rm h}z + \tfrac{1}{2}\kappa_{\rm h}^2 z^2\end{aligned} \tag{34}$$

On performing the integral over ${\rm d}^2\boldsymbol{r}$ we recover the first of equations (14).

2.4.3 Self potential of the disc

We similarly decompose the self potential energy of the into two parts, the energy $V_{\rm dd}^{\rm u}$ of an isolated flat disc, and the energy $V_{\rm dd}^{\rm w}$ associated with vertical displacements of the disc. Since $V_{\rm dd}^{\rm u}$ is fixed, it may be neglected. $V_{\rm dd}^{\rm w}$ is given by the second of equations (14).

2.4.4 Total energy

The total energy is simply the sum of the warp energy, equation (12), and the energy of the halo in the presence of an unperturbed disc:

$$E_{\rm tot} = E_{\rm warp} + E_{\rm halo}, \tag{35a}$$

where

$$E_{\rm halo} \equiv \tfrac{1}{2}\sum_{i=1}^{N_{\rm p}} m_i v_i^2 + V_{\rm hh} + V_{\rm hd}^{\rm u}. \tag{35b}$$

3 NUMERICAL DETAILS

The coupled equations of motion of the rings and particles were integrated with a symplectic leap-frog scheme that was developed according to the theory of Saha & Tremaine (1992).

3.1 Representing the disc

The disc is made up of 100 rings uniformly spaced in radius between r_1 and r_{100} with $r_{100}/r_1 = 18$. Their masses m_i are determined by the disc's surface-density profile $\Sigma_{\rm d}(r)$ and the radii r_i of the rings. In most simulations we adopted the surface density profile of Sparke & Casertano (1988):

$$\Sigma_{\rm d}(r) = \Sigma_0{\rm e}^{-r/R_{\rm d}}\times\begin{cases}1 & r\le R_{\rm t},\\ \cos^2\left(\frac{\pi}{2}\frac{(r-R_{\rm t})}{(R_0-R_{\rm t})}\right) & R_{\rm t}<r\le R_0\\ 0, & r>R_0.\end{cases} \tag{36}$$

Thus interior to $R_{\rm t}$ the disc is exponential with scale length $R_{\rm d}$, while beyond $R_{\rm t}$ its surface density tapers smoothly to zero.

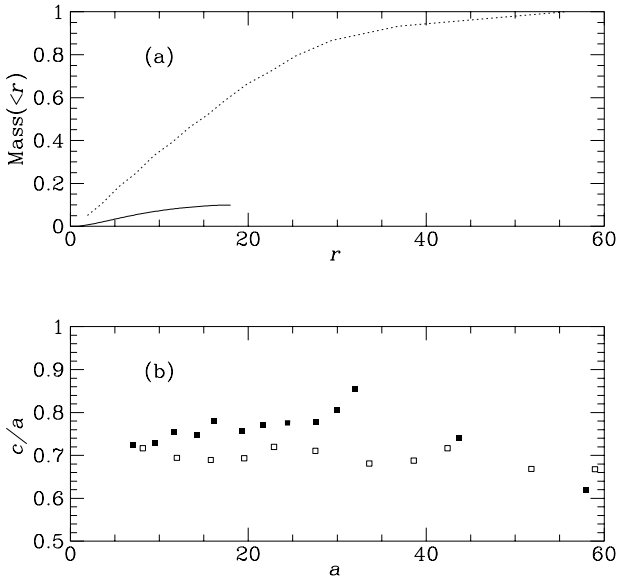

Figure 1. (a) The masses of the disc (solid curve) and the halo (dotted curve) inside a sphere of radius r. (b) The axis ratio c/a as a function of semi-major axis a. The open and full points are for the halo prior to and after insertion of the disc, respectively.

3.2 The halo

The bulge and halo are represented by $N_{\rm p} = 10^5$ particles. Since a general distribution function for a flattened halo will depend on a non-classical third integral for which no analytic expression is available, our halo model is constructed not from a distribution function but by allowing an approximate equilibrium configuration to relax towards an equilibrium. We construct an approximate equilibrium as follows. We start with a spherical system whose density profile varies approximately as r^{-2}. Specifically

$$\rho(r) = \begin{cases} \rho_0 \dfrac{{\rm e}^{-r/r_{\rm t}}}{1+r^2/r_{\rm c}^2} & \text{for } r \le r_\infty \\ 0 & \text{otherwise,} \end{cases} \tag{37}$$

where $r_{\rm c}$ is a suitable small radius, $r_{\rm t} = 50 r_{\rm c}$ and $r_\infty = 65 r_c$. The isotropic distribution function $f(E)$ of this system is obtained from Eddington's formula [eq. (4-140a) of Binney & Tremaine, 1987] and sampled by standard procedures.

This spherical system is next flattened by multiplying each z coordinate by $q < 1$. We now multiply the z-velocity of each particle by a factor α and multiply all x- and y-velocities by a factor β to ensure that the tensor virial theorem is satisfied. Specifically we require that the components T_{ii} of the kinetic-energy satisfy $2T_{ii} = -W_{ii}$, where W_{ii} is a component of Chandrasekhar's potential-energy tensor. Since $T_{zz} \propto \alpha^2$ and $T_{xx} = T_{yy} \propto \beta^2$, one easily finds that

$$\begin{aligned} \alpha^2 &= -\frac{W_{zz}}{2T^0_{zz}}, \\ \beta^2 &= -\frac{W_{xx}+W_{yy}}{4T^0_{zz}}, \end{aligned} \tag{38}$$

where T^0_{zz} is any non-vanishing component of the kinetic-energy tensor of the original spherical system.

The distribution of halo particles that has been produced as described above is only in approximate dynamical equilibrium and has yet to be modified by the gravitational potential of the embedded disc. Consequently, we integrated the equations of motion of the halo particles for a time $t_{\rm m}$ during which the mass of a flat embedded disc is ramped from zero to its final value according to the formula

$$M_{\rm d}(t) = \tfrac{1}{2}\big[1 - \cos(\pi t/t_{\rm m})\big] M_{\rm d}(t_{\rm m}), \tag{39}$$

where $t_{\rm m} = 20/\Omega(R_{\rm d})$. Fig. 1a shows for our standard model the masses of the disc and the halo that lie inside a sphere of radius r. Fig. 1b shows the axis ratio c/a of the isodensity surface in the halo that has semi-major axis a.

3.3 Scalings

Table 1 lists the numerical values of the parameters that appear in the defining equations of the disc and halo

Our unit of time is determined by these choices: (i) $r_1 = r_{\rm c} = 1$; (ii) the halo mass is unity and the disc mass is 0.1; (iii) Newton's constant $G = 1$. The circular frequency at $R_{\rm d}$ is then $\Omega(R_{\rm d}) = 0.04$ and the rms speed of halo particles is $v_0 = 0.19$. Consequently the halo's dynamical time is $t_{\rm dyn} \equiv \frac{1}{2} r_\infty / v_0 \simeq 170$.

4 RESULTS OF THE SIMULATIONS

4.1 The case of a static halo

We first check that our rings are capable of reproducing the results of Sparke & Casertano (1988) by freezing the configuration of the halo once the disc mass has been ramped up to its full value. Equation (5) of Sparke & Casertano was solved for the pattern speed $\Omega_{\rm p}$ and vertical displacement $z(r)$ of the modified tilt mode of our disc in this fixed halo. The equations of motion (11a) of the disc were then integrated from this initial condition. Fig. 2 shows that the numerical solution is exactly as it should be for a normal mode: the disc maintains it shape to high accuracy while precessing at the derived pattern speed. Fig. 3 shows that the warp energy is conserved to high accuracy – it decreases by 5 parts in 10^5 during 13 revolutions of the ring at $r = R_{\rm d}$.

These results demonstrate that we have accurately modelled the disc–halo interaction and are correctly following the dynamics of the disc.

4.2 Forced precession of the disc

Next we check the calculation of Nelson & Tremaine (1995) by evolving the halo while the disc is caused to precess at a steady rate in a given warped configuration. The latter was the approximate normal-mode configuration considered by Nelson & Tremaine.

Fig. 4 shows the consequent evolution of the halo energy that is defined by equation (36). The disc's warp energy is $E_{\rm warp} \simeq 3\times10^{-4}$, so, in so far as the straight line of slope $\dot E_{\rm h} = 2.8\times10^{-7}$ that is plotted in Fig. 5 provides an adequate approximation to the dependence of $E_{\rm halo}$ on time, the decay rate of the warp is $\Gamma = \dot E_{\rm halo}/E_{\rm warp} = 9\times10^{-4}$ and $\Gamma/\Omega(R_{\rm d}) = 0.02$. This value of Γ lies exactly in the middle of the range of values for the same quantity that Nelson & Tremaine plot in their Fig. 2.

This calculation suggests both that we are integrating the equations of motion of the halo particles accurately, and that the approximations employed by Nelson and Tremaine to estimate the effect of the warp on the halo are not misleading.

Table 1. Parameters

Disc						Halo			
r_1	r_{100}	R_d	R_t	R_0	M_d	r_c	r_t	r_∞	M_h
1	18	4.5	15.75	18	0.1	1	50	65	1

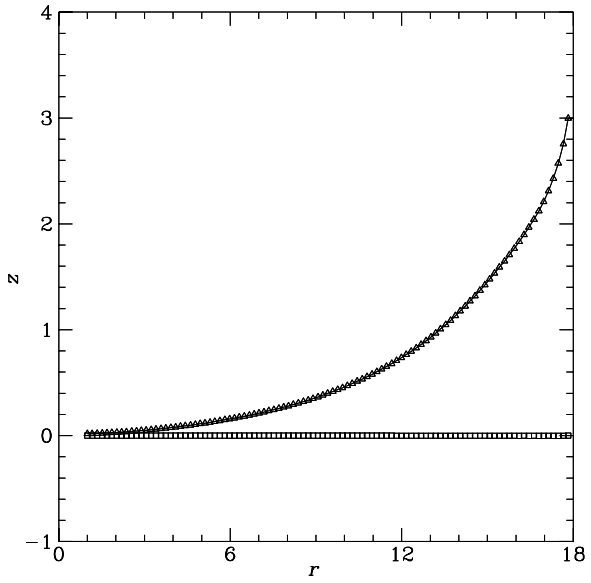

Figure 2. Plots of $z(t, r, \phi = \Omega_\mathrm{p} t)$ for $t = 0$ (curve) and $t = 2000$ (triangles) when the disc is allowed to evolve from the configuration of a normal-mode for time t in a frozen halo ($2000\Omega_\mathrm{p} = 164°$). The open squares show $z(t, r, \phi = \Omega_\mathrm{p} t + \frac{1}{2}\pi)$ at $t = 2000$. (The corresponding values of z for $t = 0$ are identically zero.)

4.3 A live disk in a live halo

Fig. 5 shows the evolution of the curve of nodes of live disc that evolves in a live halo from an initial condition that is a normal-mode in the sense of Sparke & Casertano. It is apparent that the warp winds up within a few dynamical times. Fig. 6 shows, as a function of time, the rms vertical displacement $|z| = (z_\mathrm{c}^2 + z_\mathrm{s}^2)^{1/2}$ for this simulation. This does not evolve dramatically. Only in the innermost third of disc is there any tendency for the rms displacement to decrease with time. In the outermost quarter of the disk the rms displacement clearly increases slightly through the duration of the simulation. It turns out that the growth in $|z|$ at large radii predominates in the sense that E_warp tends to increase.

5 CONCLUSIONS

We have used a program that uses rings to represent the disc and particles to represent the halo to model the dynamics of a disc that is embedded in a live massive halo. We have checked the correctness of the program as regards the disc and its interaction with the halo by showing that when the halo is frozen, and the disc is started in a Sparke–Casertano normal mode, it precesses rigidly as the normal-mode calculations require. We have checked the correctness of the program as regards the halo by showing that when the disc is rigid and forced to precess at a constant rate, the halo acquires energy at the rate predicted by Nelson & Tremaine (1995).

When the halo is live and the disc is started from the configuration of a normal mode, the warp is not rapidly damped as

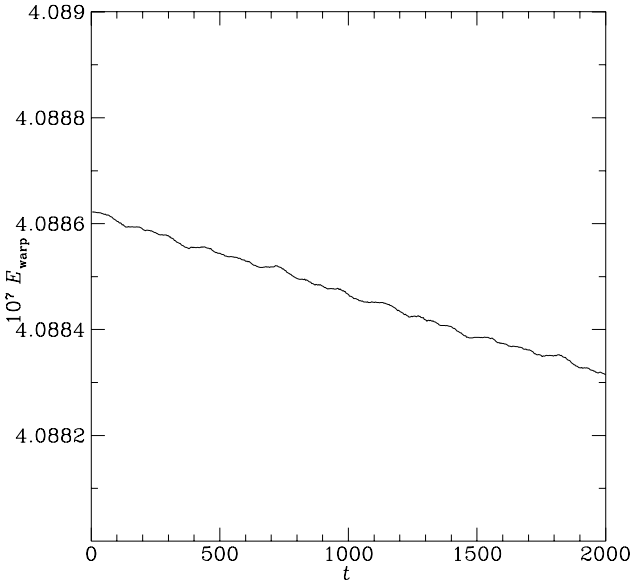

Figure 3. Warp energy [equation (12)] as a function of time for a disc evolving in a frozen halo.

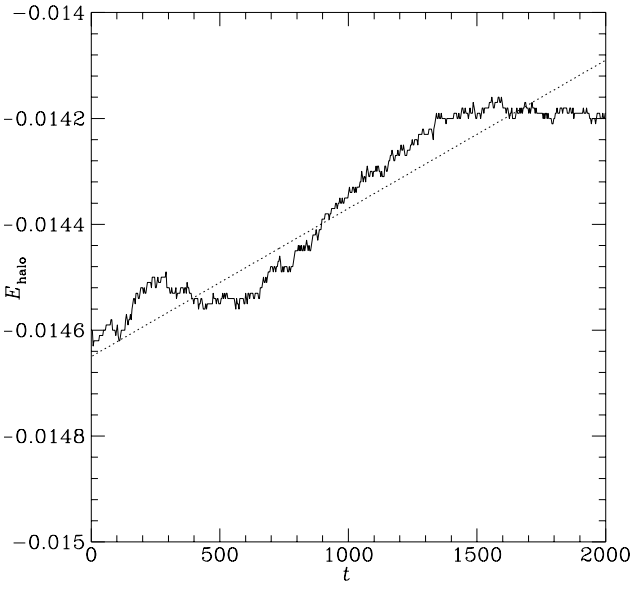

Figure 4. The energy of the halo [equation (36)] when a warped disk is forced to precess at a constant rate. The dotted line is the fit used in the text. Notice that $E_\mathrm{warp}/E_\mathrm{halo} \sim 0.02$, so calculating energies to the required accuracy is computationally challenging.

Nelson & Tremaine predicted, but winds up within a few dynamical times, whilst retaining or even enhancing its 'warp energy'. How may this result be understood?

We have to consider two distinct dynamical systems: (a) the disc in a frozen halo, and (b) the disc in a live halo. Let us call (a) the Frozen System and (b) the Live System. The tight coupling between the disc and halo that is demonstrated by the calculation of Nelson & Tremaine already implies that the normal modes of the live system are not close to the normal modes of the

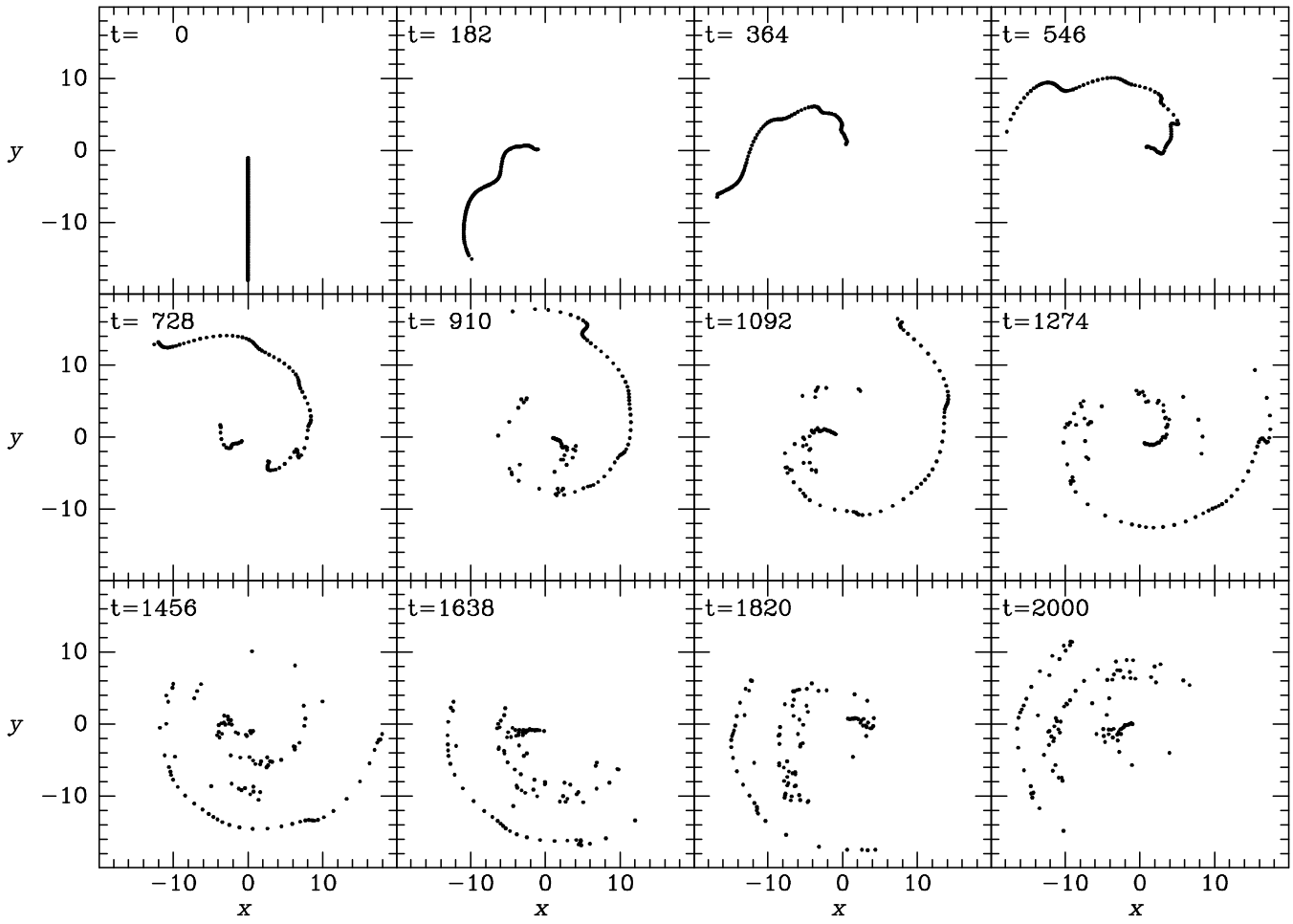

Figure 5. A warp in a live halo rapidly winds up even though its initial configuration would be a normal mode if the halo were static. Here we plot at several times the curve of nodes that is defined by $\phi(r) = \pi + \mathrm{atan2}[z_{\rm c}(r), -z_{\rm s}(r)]$ for a live disc that evolved in a live halo from a configuration that was a normal mode in the sense of Sparke & Casertano.

frozen system. Hence, if we were to express the configuration that corresponds to any low-order normal mode of the frozen system as a linear combination of normal modes of the live system, the sum would not be dominated by a single term. The configuration described by the sum would evolve significantly on a timescale that is inversely proportional to the biggest frequency difference $\Delta\omega_{\rm max}$ between the normal modes that have non-negligible amplitudes in the sum. The rapidity with which a warp of the live system winds up from a normal-mode configuration of the frozen system implies that $\Delta\omega_{\rm max}$ is large.

To understand why this should be so, consider the probable form of the normal modes of the live system. At any radius the density of the halo has a strong tendency to peak at the vertical location of the disc, because the latter is extremely dense. Equivalently, a substantial input of energy is required to displace the disc from the halo's local equator. By contrast, relatively little energy is required to tip the outer disc and halo with respect to the inner disc and halo – the outer and inner parts of a flattened galaxy are kept in angular alignment principally by the interaction between the mass quadrupole of the outer galaxy with the inner galaxy's potential quadrupole, which is attenuated by the cube of the ratio of the characteristic radii of the inner and outer parts of the galaxy.

Now it is generally true that deformations of a system that are associated with small energy increments are associated with low-frequency normal modes, while those that are associated with large energy increments are associated with high-frequency normal modes. So a normal mode that displaces the disk from the local equator of the halo will have a much higher frequency than one that tips the outer parts of the galaxy with respect to the inner parts.

To generate a normal mode of the frozen system we have to do two things: First, we generate the warp in the disc by rotating the outer galaxy with respect to the inner galaxy. Then, we eliminate the twist just introduced into the halo by displacing the halo with respect to the disc at both large and small radii. Thus, when expressed as a sum over normal modes of the live system, a normal mode of the frozen system involves both high-frequency and low-frequency terms in an essential way. From this it follows that it will wind up rapidly, essentially at the frequency of the high-frequency normal modes.

The argument we have just given explains why our initial warped configurations rapidly wind up. It also suggests that true normal modes of the full live system may involve configurations of the *disc* that are very similar to those of Sparke–Casertano normal modes. It is in their *halo* configurations that these true normal modes would differ essentially from Sparke-Casertano normal modes. It is likely that these differences in halo structure will give rise to the true normal modes having significantly lower frequencies than do Sparke-Casertano normal modes. We hope soon to return to this prediction.

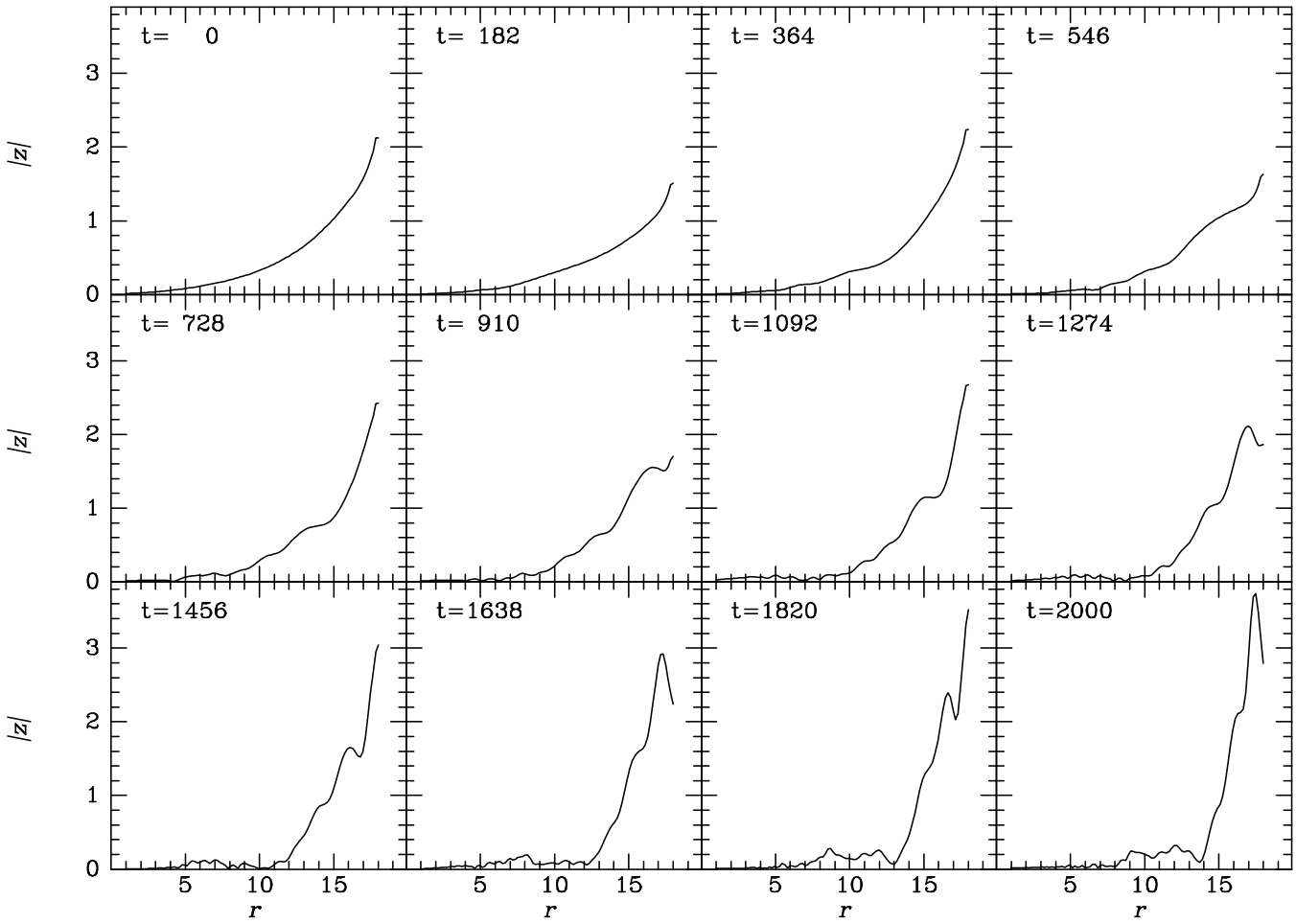

Figure 6. The rms vertical displacement $|z| = (z_c^2 + z_s^2)^{1/2}$ as a function of radius for the simulation whose curves of nodes are shown in Fig. 5.

REFERENCES

Binney J., 1992, ARA&A, 30, 51
Binney, J., & Tremaine, S., 1987, Galactic Dynamics, Princeton University Press, Princeton
Dekel A., Shlosman I., 1983, in IAU Symposium 100, 'Internal Kinematics and Dynamics of Galaxies', ed. E. Athanassoula, Dordrecht, Reidel, p. 187
Dubinski J., Kuijken K., 1995, ApJ, 442, 492
Fich M., Tremaine S.D., 1991, ARA&A, 29, 409
Hunter C., Toomre A., 1969, ApJ, 155, 747
Kent S.M., Dame T.M., Fazio G., 1991, ApJ, 378, 131
Nelson R.W., Tremaine S., 1995, MNRAS, 275, 897
Nelson R.W., Tremaine S., 1996, in 'Gravitational Dynamics', eds O. Lahav E. Terlevich and R.J. Terlevich, Cambridge University Press, Cambridge, p. 73
Saha P., Tremaine S.D., 1992, AJ, 104, 163
Sparke L.S., Casertano S., 1988, MNRAS, 234, 873
Toomre, A., 1983, in IAU Symp. 100, 'Internal Kinematics and Dynamics of Galaxies', ed. E. Athanassoula, Reidel, Dordrecht, p. 177

This paper has been produced using the Blackwell Scientific Publications TEX macros.